are in different orientations in the cyclamer.

Conclusions

This work has shown that 1,3-cyclohexanedione (CHD) forms stereoisomeric hydrogen-bonded supermolecules in the solid state. One of these supermolecules is a cyclic structure, called a cyclamer, which serves as a host in complexing benzene, perdeuteriobenzene, and monodeuteriobenzene. CHD monomers, which are enolic, form supermolecules by aggregating via strong intermolecular hydrogen bonds with O···O hydrogen-bond distances of 2.51–2.57 Å, nearly as short as the O···O intramolecular hydrogen-bond contacts found in acyclic β-diketomethanes. High-resolution solid-state NMR spectroscopy and X-ray crystallography were used as complementary tools to elucidate the structures of the host-guest complexes and the dynamic properties of the included guest species.

Acknowledgment. We gratefully acknowledge the crystallographic assistance of Prof. Doyle Britton, University of Minnesota, and Thomas Panunto who assisted with X-ray powder pattern experiments. We also acknowledge the services of the Colorado State University Regional NMR Center, funded by the National Science Foundation Grant No. CHE-8208821, and support from the Olin Corporation Charitable Trust Grant of the Research Corporation to M.C.E.

Registry No. I, 504-02-9; II, 103620-43-5; IV, 103620-45-7; C_6D_6·61, 103620-44-6.

Supplementary Material Available: Tables 1 and 2 listing fractional atomic coordinates and anisotropic thermal parameters for compounds I and II (2 pages); tables of calculated and observed structure factors (9 pages). Ordering information is given on any current masthead page.

Electrocatalytic Reduction of Nitrite to Ammonia Based on a Water-Soluble Iron Porphyrin

Mark H. Barley, Kenneth J. Takeuchi, and Thomas J. Meyer*

Contribution from the Department of Chemistry, The University of North Carolina, Chapel Hill, North Carolina 27514. *Received November 21, 1985*

Abstract: In aqueous solution at either pH 4.5 or 6.7, the water-soluble porphyrin $[Fe^{III}(H_2O)(TPPS)]^{3-}$ (H_2TPPS^{4-} = tetraanonic form of *meso*-tetrakis(*p*-sulfonatophenyl)porphyrin) is an effective electrocatalyst for the reduction of nitrite ion to ammonia with hydroxylamine or N_2O also appearing as significant products, depending upon the reaction conditions. The reductions proceed via the nitrosyl complex $[Fe^{II}(NO^+)(TPPS)]^{3-}$ as an intermediate. The nitrosyl complex forms at pH <3.0 by a reaction between the Fe(III) porphyrin and NO arising from disproportionation of HONO or, at 4.0 < pH >7.0, following reduction of Fe(III) to Fe(II) ($E_{1/2}$ = −0.23 V vs. SSCE) via an acid-base reaction. Reduction of the nitrosyl complex occurs by sequential 1-electron steps at $E_{1/2}$ = +0.35 and −0.63 V vs. SSCE, the second of which is pH-dependent at pH <2.6. Evidence for a third 1-electron step has been found by differential pulse polarography at pH 2.1. The first two reductions are followed by a multiple-electron wave which is greatly enhanced as the pH is decreased from 4 to 2.6. Although NH_3 is the ultimate reduction product at −0.9 V, NH_2OH appears to be an intermediate stage in the reduction and electrolysis to the 2-electron stage at −0.63 V gives increasing yields of N_2O. The redox properties of the nitrosyl complex and probable mechanism of reduction of NO_2^- to NH_3 are discussed and compared with earlier results obtained on polypyridyl complexes of Os and Ru.

The enzyme nitrite reductase (found in bacteria, fungi, and plants) converts nitrite to ammonia in a net 6-electron, five-proton reduction process.[1] The enzyme utilizes an iron isobacteriochlorin as the active site. Chlorins, bacteriochlorins, and isobacteriochlorins are all derived from a parent porphyrin by the hydrogenation of one or two pyrrollic double bonds.[2] One line of current research has emphasized the study of synthetic iron isobacteriochlorins and related complexes in order to determine the distinctive features of the active site that allow it to catalyze the reduction of nitrite.[3] However, recent results have shown that a number of simple iron complexes are capable of reducing NO catalytically to ammonia,[4] suggesting that the key to the redox chemistry may lie in the Fe-NO fragment and be relatively insensitive to the nature of the additional ligands coordinated to the iron center.

Studies of the reductive chemistry of the bound nitrite and nitrosyl ligands have concentrated on the stoichiometric or near stoichiometric reduction of these ligands coordinated to Fe, Ru, or Os.[5,6] Results obtained for polypyridine complexes of ruthenium and osmium have demonstrated the facile interconversion of bound nitrite and nitrosyl[7] and also the chemical and electrochemical reduction of bound nitrosyl to coordinated ammonia.[5,6] The results of detailed electrochemical studies have allowed a mechanism to be proposed based on a series of 1-electron reductions, initially at the nitrosyl ligand, which lead to a series of detectable intermediates.[6]

There are numerous examples in the literature of iron nitrosyl porphyrins,[8] and detailed electrochemical studies on the complexes Fe(NO)(TPP) and Fe(NO)(OEP) (OEP^{2-} = dianion of octaethylporphine, TPP^{2-} = dianion of *meso*-tetraphenylporphine) in

(1) Losada, M. *J. Mol. Catal.* **1975**, *1*, 245-265.
(2) (a) Scheer, H. *The Porphyrins*; Dolphin, D., Ed.; Academic Press: New York, 1979; Vol. II, Chapter 1. (b) Bonnet, R. *Ibid.* Vol. 1, Chapter 1.
(3) (a) Chang, C. K.; Fajer, J. *J. Am. Chem. Soc.* **1980**, *102*, 848. (b) Chang, C. K., Hanson, L. K.; Richardson, P. F.; Yound, R.; Fajer, J. *Proc. Natl. Acad. Sci. U.S.A.* **1981**, *78*, 2652. (c) Stolzenberg, A. M.; Strauss, S. H.; Holm, R. H. *J. Am. Chem. Soc.* **1981**, *103*, 4763. (d) Strauss, S. H.; Silver, M. E.; Ibers, J. A. *J. Am. Chem. Soc.* **1983**, *105*, 4108. (e) Fujita, E. Fajer, J. *J. Am. Chem. Soc.* **1983**, *105*, 6743.
(4) (a) Uchiyana, S.; Muto, G. *J. Electroanal. Chem.* **1981**, *127*, 275. (b) Ogwa, K.; Ishikawa, H. *J. Chem. Soc., Faraday Trans. 1* **1984**, *80*, 2243.
(5) (a) Bottomley, F.; Mukaida, M. *J. Chem. Soc., Dalton Trans.* **1982**, 1933. (b) Armor, J. N.; Hoffman, M. Z. *Inorg. Chem.* **1975**, *14*, 444. (c) Armor, J. N. *Inorg. Chem.* **1973**, *12*, 1959.
(6) (a) Murphy, W. R., Jr.; Takeuchi, K. J.; Meyer, T. J. *J. Am. Chem. Soc.* **1982**, *104*, 5818. (b) Murphy, W. R., Jr.; Takeuchi, K. J.; Barley, M. H.; Meyer, T. J. *Inorg. Chem.*, in press.
(7) Godwin, J. B.; Meyer, T. J. *Inorg. Chem.* **1971**, *10*, 2150.
(8) Buchler, J. W. In *The Porphyrins*; Dolphin, D., Ed.; Academic Press: New York, 1979; Vol. I, p 458.

0002-7863/86/1508-5876$01.50/0

benzonitrile have appeared.[9] In nonaqueous solvents a series of 1-electron reductions are observed which, given the potentials involved, appear to be localized at Fe-NO levels.

We report here our work on the redox properties of solutions containing the water-soluble porphyrin $[Fe^{III}(TPPS)]^{3-}$ (H_2TPPS^{4-} = tetraanionic form of *meso*-tetrakis(*p*-sulfonatophenyl)porphine) and nitrite in aqueous solution. We find that a nitrosyl complex forms in aqueous solution and that in water, where the proton demands of the net reaction can be met, further reductions are observed past the 2-electron stage and the system acts as an electrocatalyst for the reduction of nitrite to ammonia. A preliminary account of our results has appeared elsewhere.[10]

Experimental Section

Materials. Argon was purchased from Linde. Nitric oxide was obtained from Matheson and diluted by mixing with a fast flowing argon stream.

Phosphate buffer solutions were prepared from locally deionized water which had been distilled from alkaline permanganate. Buffer solutions (pH >2) consisted of 0.1 M solutions of phosphate mixtures (H_3PO_4, KH_2PO_4, and Na_2HPO_4) with small pH adjustments made by using 0.1 M H_2SO_4 or 0.1 M NaOH. For pH <2, the pH was controlled by 0.1 M $H_2SO_4/NaHSO_4$ mixtures. In some of the electrochemical experiments 0.6 M Na_2SO_4 was added to the buffer to improve the charge-transfer characteristics of the redox couples. For controlled-potential electrolysis experiments the buffer concentration was increased to 0.5 M to limit the pH change during the catalytic reduction.

$[Fe^{III}(TPPS)^{3-}$,3Na^+·12H_2O. The water-soluble porphyrin was synthesized as the sodium salt by a modification of the method described by Fleischer and Taniguchi.[11,12] $[H_2TPPS]^{4-}$,4Na^+·12H_2O (Strem), 415 mg, was dissolved in warm (60–80 °C) water, 10 equiv of $Fe^{II}SO_4$·7H_2O were added, and the mixture was heated for about 20 min after the addition of 2 equiv of NaOH. The sample was purified while in solution by cation exchange and separated from Na_2SO_4 by methanol extraction as described by Taniguchi.[12] Yield 361 mg, 85%. Anal. Found: C, 41.25%; H, 3.69%; N, 4.38%. Theoretical: C, 41.55%; H, 3.80%; N, 4.45%.

Techniques and Instrumentation. Vitreous carbon working electrodes were fabricated from Tokai carbon and encapsulated in a Teflon sheath by techniques previously described.[13] The electrodes were used either freshly polished[6b] or after activation by a literature procedure.[14] The reference electrode was a saturated sodium chloride calomel electrode (SSCE, +0.234 V vs. NHE[15]) with a cellulose junction. Auxiliary electrodes were platinum wires or platinum mesh for the bulk electrolysis experiments.

Electrochemical cells for cyclic voltammetry (CV) and differential pulse polarography (DPP) experiments were plain glass containers equipped with Teflon tops of various designs to hold the electrodes and to limit the access of air to the solution. Mercury (triply distilled, from Bethlehem Apparatus Co.) was used without further purification for working electrodes in the bulk electrolyses. Porous Vycro glass (no. 7930) was obtained from Corning and cut to the required length. Gas-tight cells for bulk electrolysis were fabricated from a plain glass container and a Teflon top equipped with an O-ring.

The cyclic voltammetric (CV) and differential pulse polarographic (DPP) experiments were carried out by using a PAR 174 potentiostat in conjunction with a home-made programmer to generate the triangle waveforms. Controlled-potential electrolyses (catalytic runs) were done with a PAR Model 173 potentiostat/galvanostat with a PAR Model 179 digital coulometer. The current-time or current-potential curves were recorded on a Hewlett-Packard Model 7015B X-Y recorder. pH measurements were made by using a Radiometer digital pH meter after calibration using Fisher buffers. UV/visible absorption spectra were recorded on a Bausch & Lomb Spectronic 2000 spectrophotometer.

Table I. Visible Spectral Data in Water for the Iron-TPPS Complexes and for TPP Analogues in Nonaqueous Solvents

complex	λ_{max}, nm ($\log_{10}\epsilon$, M^{-1} cm^{-1})
$[Fe^{III}(H_2O)(TPPS)]^{3-}$ (**2**)	393 (5.19), 528 (4.09), 680 (3.38)
$[Fe^{III}(TPPS)]_2O^{8-}$ [a] (**3**)	408 (5.37), 567 (4.17), 607 (3.91)
$[Fe^{II}(NO^+)(TPPS)]^{3-}$ (**4**)	355 (4.68), 425 (5.14), 540 (4.08), 576 (3.59) sh
$[Fe^{II}(NO^+)(TPP)]^+$ [b]	410 (5.00), 423 (4.99), 539 (4.06), 570 (2.90)
$[Fe^{II}(NO^·)(TPPS)]^{4-}$ (**5**)	410 (4.96), 542 (3.90), 602 (3.63)
$[Fe^{II}(NO^·)(TPP)]$ [b]	410 (5.04), 540 (3.95), 610 (3.60)
$[Fe^{II}(H_2O)_n(TPPS)]^{4-}$ (**6**)	424 (5.29), 556 (4.03), 594 (3.80)
$[Fe^{II}(THF)_2(TPP)]$ [c]	424 (5.49), 539 (4.08), 553 (4.04)

[a] Spectrum agrees with the results of Taniguchi, ref 12. [b] In benzonitrile, ref 9b. [c] In THF: Reed, C. A.; Mashiko, T.; Scheidt, W. R.; Spartaliar, K.; Lang, G. *J. Am. Chem. Soc.* **1980**, *102*, 2302.

Preparation of solutions containing iron(II) porphyrins for spectroscopic studies utilized Schlenck tubes and vigorous argon purging of the iron(III) porphyrin solution prior to reduction. Alternatively, solutions of the iron(III) porphyrin were transferred to a 1-mm optical cell fitted with a septum and solutions of the reducing agent were added via a microliter syringe.

The products of catalysis were assayed by a combination of GC and ^{14}N NMR techniques. The GC used was a Hewlett-Packard 5890A gas chromatograph equipped with a thermal conductivity detector. Nitrogen was assayed on a molecular sieve column using air as the standard. Nitrous oxide was assayed on a Porapak Q column[16] and the estimated volume corrected for the solubility of the gas in aqueous solutions.[17] Ammonia was analyzed by GC, using a Chromosorb 103 column (all columns obtained from Alltech Associates) at an elevated temperature after adding sufficient NaOH to bring the pH of the solution to 10. A 0.01 M solution of ammonium sulfate (0.02 M NH_4^+) in phosphate buffer at the same pH was used as a standard. The presence of hydroxylamine in some of the samples, and the absence of hydrazine, was demonstrated by ^{14}N NMR, using a Bruker 250-MHz spectrometer. Resonances were identified by comparison of peak positions both with those of standard samples and with values reported in the literature.[18] Due to complications arising from ^{14}N nuclear spin relaxation, integration of the ^{14}N signals could not be used for quantitative analyses, and N_2, N_2O, and ammonia were determined directly by GC; the remaining reducing equivalents were assumed to be present as hydroxylamine. Independent corroboration of hydroxylamine as a product was established in one experiment using high $[NO_2^-]$/porphyrin ratios and a limited electrolysis period in order to maximize NH_2OH formation. Note the results of experiment 5 in Table III. A trace amount of catalyst was used and the hydroxylamine concentration determined using a specific colorimetric test.[19] The colorimetric procedure was carried out after removal of the phosphate buffer by precipitation with Ca^{2+}. Phosphate was precipitated out at pH >6 by using $CaCl_2$(sat). In the process the solution was diluted by a factor of 2. A portion of the solution was acidified to pH ~3 and a solution containing the colorimetric reagents added in the ratio 4:1. After 5 min the expected deep red color was fully developed and gave an absorbance at 511 nm = 0.69. A similar series of dilutions was executed on a blank solution of 0.01 M $[NH_3OH]Cl$ giving A(511 nm) = 0.88. After correction for the amount of excess Fe^{III} added in the colorimetric procedure,[19] the solution contained $\sim 7.7 \times 10^{-3}$ M hydroxylamine consistent with the appearance of ~80% of the nitrite produced as hydroxylamine. That N_2, N_2O, and NH_3 were minor products was verified by GC and ^{14}N NMR.

Results

Before considering the reduction of NO_2^- to NH_3 it is necessary to define in some detail the background solution and electrochemical properties of the metalloporphyrin catalyst.

Solution Chemistry of $[Fe^{III}(TPPS)]^{3-}$,3Na^+·12H_2O (1). Dilute aqueous solutions of the sodium salt are deep orange/brown in color (Table I) at pH <7. The solutions are thought to contain

(9) (a) Olson, L. W.; Schaeper, D.; Lancon, D.; Kadish, K. M. *J. Am. Chem. Soc.* **1982**, *104*, 2042. (b) Lancon, D.; Kadish, K. M. *J. Am. Chem. Soc.* **1983**, *105*, 5610.

(10) Barley, M. H.; Takeuchi, K.; Murphy, W. R., Jr.; Meyer, T. J. *J. Chem. Soc., Chem. Commun.* **1985**, 507.

(11) Fleischer, E. B.; Palmer, J. M.; Srivastava, T. S.; Chatterjee, A. *J. Am. Chem. Soc.* **1971**, *93*, 3162.

(12) Taniguchi, V. T. Ph.D. Thesis, University of California, Irvine, 1978.

(13) Martin, G. W. Ph.D. Dissertation, University of North Carolina, 1978.

(14) (a) Diamantis, A. A.; Murphy, W. R. Jr.; Meyer, T. J. *Inorg. Chem.* **1984**, *23*, 3230. (b) Cabaniss, G. E.; Diamantis, A. A.; Murphy, W. R., Jr.; Linton, R. W.; Meyer, T. J. *J. Am. Chem. Soc.* **1985**, *107*, 1845-1853.

(15) Bard, A. J.; Faulkner, L. R. *Electrochemical Methods*; Wiley: New York, 1980; end pages.

(16) Thomas, B. *Fundamentals of Gas Analysis by Gas Chromatography*; Varian, 1977.

(17) *Handbook of Chemistry and Physics*, 55th ed.; Weast, R.C., Ed.; CRC Press: Cleveland, OH, 1974; p B-115.

(18) Emsley, J. W.; Ferney, J.; Sutcliff, L. H. *High Resolution Nuclear Magnetic Resonance Spectroscopy*; Pergamon Press: New York, 1966; Vol. 2, Chapter 12.

(19) Feigel, F.; Anger, V. *Spot Tests in Inorganic Chemistry*; Elsevier: New York, 1972; p 344.

Table II. $E_{1/2}$ Values for Fe(TPPS) Couples and Their TPP Analogues vs. SCE

$TPPS^{4-}$ couples	$E_{1/2}$, V	TPP couples	$E_{1/2}$, V
$[Fe^{III}(H_2O)TPPS]^{3-}$ (2)			
$[Fe^{III}(H_2O)TPPS]^{3-}/[Fe^{II}(H_2O)_2TPPS]^{4-}$	-0.23[a]	$Fe^{III}(TPP)Cl/Fe^{II}(TPP)$	-0.34[b]
$[Fe^{III}(H_2O)(TPPS^{\cdot+})]^{2-}/[Fe^{III}(H_2O)(TPPS)]^{3-}$	+0.93[a]	$[Fe^{III}(TPP^{\cdot+})Cl]^{+}/Fe^{III}(TPP)Cl$	+1.11[c]
$[Fe^{II}(H_2O)_nTPPS]^{4-}/[Fe^{I}(TPPS)]^{5-}$	-1.12[a]	$Fe^{II}(TPP)/[Fe^{I}(TPP)]^{-}$	-1.03[b]
$[Fe^{II}(NO^{+})(TPPS)]^{3-}$ (4)			
$[Fe^{II}(NO^{+})(TPPS)]^{3-}/[Fe^{II}(NO^{\cdot})(TPPS)]^{4-}$	+0.35[d]	$[Fe(NO)TPP]^{+}/Fe(NO)TPP$	+0.75[f]
$[Fe^{II}(NO^{\cdot})(TPPS)]^{4-}/[Fe^{II}(NO^{-})(TPPS)]^{5-}$	-0.63[e]	$Fe(NO)TPP/[Fe(NO)TPP]^{-}$	-0.88[f]
$[Fe^{III}(TPPS)]_2O^{8-}$ (3)		$[Fe^{III}(TPP)]_2O$	
first ring oxidation	~+0.6	first ring oxidation	+0.83[c]
second ring oxidation	~+0.8	second ring oxidation	+1.09[c]

[a] 0.1 M H_2SiSO_4. [b] In THF from ref 28a. [c] In CH_2Cl_2 from ref 22. [d] 0.1 M phosphate buffer + 0.6 M Na_2SO_4, $[NO_2^-] = 2 \times 10^{-2}$ M, porphyrin at 2×10^{-3} M. [e] pH >2.6; 0.1 M phosphate + 0.6 M Na_2SO_4, porphyrin at $\sim 4 \times 10^{-4}$ M, $[NO_2^-] = 2 \times 10^{-3}$ M. [f] Reference 9b, in benzonitrile.

the aquo ion $[Fe^{III}(H_2O)_n(TPPS)]^{3-}$ (2) where $n = 1$ or 2, but n is more likely to be 1, with the pentacoordinate d^5 iron ion in the high spin state.[20] In alkaline solution the deep green μ-oxo dimer $[[Fe^{III}(TPPS)]_2O]^{8-}$ (3) (Table I) is formed,[12] via

$$[Fe^{III}(H_2O)(TPPS)]^{3-} + OH^- \rightarrow [Fe^{III}(OH)(TPPS)]^{4-} + H_2O \quad (1)$$

$$2[Fe^{III}(OH)(TPPS)]^{4-} \rightarrow [[Fe^{III}(TPPS)]_2O]^{8-} + H_2O \quad (2)$$

Dimer formation at approximately millimolar monomer concentration is greatly favored by increased ionic strength. Hence the dimer is formed at pH >6 in 0.1 M buffer solutions, but the addition of 0.6 M Na_2SO_4 causes dimerization to occur at pH >3.5. The ionic strength dependence of dimer formation is not surprising considering the charge types involved.

It has been reported that aqueous solutions of metallo complexes of H_2TPPS^{4-} show deviations from Beer's law suggesting aggregation.[21] With analytically pure samples of **2**, Beer's law was obeyed under conditions expected to promote aggregation (0.1 M H_2SO_4/0.6 M Na_2SO_4) over the concentration range 10^{-6} to 3×10^{-3} M. The result suggests that under the conditions of our experiments there are no complications from aggregation of the porphyrin complex.

Electrochemistry of $[Fe^{III}(H_2O)(TPPS)]^{3-}$ (2). A cyclic voltammogram of **2** is shown in Figure 1a. The wave at $E_{1/2} = -0.23$ V is a metal-based Fe(III)/Fe(II) reduction which even under favorable conditions (see below) still shows a peak splitting (ΔE_p) of ~200 mV, consistent with slow heterogeneous charge transfer. The shape of the voltammogram is very sensitive to solution composition and the nature of the electrode surface. Well-defined waves at $E_{1/2} = -0.23$ V were obtained at polished carbon electrodes in the presence of 0.6 M Na_2SO_4 or by using an activated carbon electrode[14] with 10^{-3} M solutions of **2** in 0.1 M H_2SO_4.[22]

For the metal-centered redox process, plots were made of $i_p/v^{1/2}$ vs. $v^{1/2}$ (Figure 2A) and of ΔE_p vs. $v^{1/2}$ (Figure 2B) for 10^{-3} M solutions of **2** in the presence of either 0.1 M H_2SO_4 with added 0.6 M Na_2SO_4 or in 0.1 M H_2SO_4 alone by using an activated carbon electrode. v is the scan rate in millivolts, i_p is the oxidative peak current, and ΔE_p is the difference in peak potentials between the reductive and oxidative peaks. The plots show that both the current function ($i_p/v^{1/2}$) and peak potential difference are dependent on scan rate, confirming the quasi-reversible nature of the reduction of Fe(III) to Fe(II). Qualitatively, the rate of heterogeneous charge transfer (k_s) is sensitive to both electrolyte composition and the pretreatment of the carbon electrode.[14]

The peak potential for the $[Fe(H_2O)_n(TPPS)]^{3-/4-}$ ($n = 1$ or 2) wave at -0.23 V with added 0.6 M Na_2SO_4 is independent of pH over the range $1.0 < pH < 7.0$. The independence of pH taken with Taniguchi's estimate of a $pK_a = 8.1$ for the aqua Fe(III) form of the porphyrin[12] shows that in the pH range used in our experiments ($1.0 < pH < 7.0$) both the iron(II) and iron(III) complexes contain H_2O rather than hydroxy groups in the axial positions.

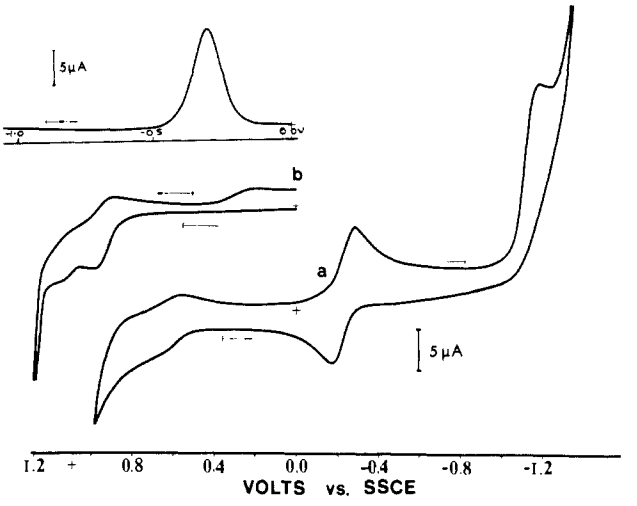

Figure 1. Cyclic voltammograms (100 mV/s) and differential pulse polarogram (10 mV/s, inset) of a solution 10^{-3} M in $[Fe^{III}(H_2O)(TPPS)]^{3-}$, 0.6 M in Na_2SO_4, and 0.1 M in buffer, vs. SSCE. (a) Steady-state CV at a polished electrode at pH 3.55; (b) CV at an activated electrode at pH 1.44 showing an extension of the scan into the porphyrin oxidation region. Note the change in potential scale for the differential pulse polarogram. The wave shown corresponds to the Fe(III)/(II) wave in the cyclic voltammogram.

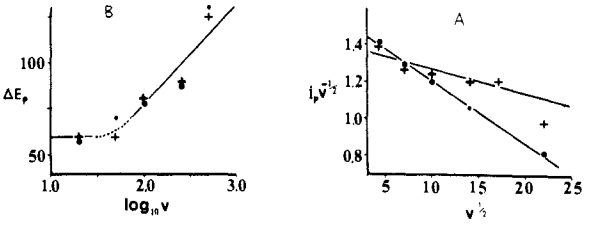

Figure 2. (A) Plot of $i_p v^{-1/2}$ vs. $v^{1/2}$ (i_p is the reductive peak current and v the scan rate in mV/s) for the Fe(III)/(II) couple at a polished electrode in 0.1 M H_2SO_4 with added 0.6 M Na_2SO_4 (+) or at an activated carbon electrode[14] in 0.1 M H_2SO_4 (●). $[Fe^{III}(H_2O(TPPS)^{3-}] = 1 \times 10^{-3}$ M. (B) Same conditions showing a plot of ΔE_p (the potential difference between the oxidative and reductive peak currents) vs. $\log_{10} v$.

(20) Reference 12, pp 393-394.
(21) Harriman, A.; Porter, G.; Walters, P. *J. Chem. Soc., Faraday Trans. 2* **1983**, *79*, 1335.
(22) Electrochemical studies on dilute solutions (~10^{-4} M) of some samples of $[Fe^{III}(H_2O)(TPPS)]^{3-}$ (**2**) gave evidence for the presence of an impurity which preferentially absorbed onto the carbon electrode. The amount of impurity varied between samples but never accounted for more than ~4% of the total current as estimated by cyclic voltammetry. The presence of the impurity is more obvious in the DPP experiments apparently because its redox processes are more reversible than those of **2**. For the impurity a single peak was observed at $E_p = -0.1$ V in a solution containing 0.1 M buffer and 0.6 M Na_2SO_4 at pH >1.7. In a similar solution but at a pH <1.7 the peak disappears and is replaced by two peaks at $E_p = -0.48$ and -0.70 V. Evidence for the preferential absorption of the impurity on the electrode surface was obtained by transferring an electrode from a solution 5×10^{-4} M in porphyrin to a solution containing electrolyte alone. Waves due to the impurity were still observed in the fresh solution but are soon lost as the material diffuses from the electrode surface. At porphyrin concentrations >1×10^{-3} M with use of a freshly polished carbon electrode, the impurity waves were usually not observed. Upon addition of nitrite (see below) the impurity peaks also disappear. From our observations, we conclude that the impurity is not involved or plays an unsignificant role in the nitrite reduction chemistry described below.

A further oxidation of **2** (Figure 2) occurs at +0.93 V (pH 1.4, 0.1 M H_2SO_4 + 0.6 M Na_2SO_4) which is pH-independent (1.0 < pH < 4.0). Although not of particular interest here, the results of a series of experiments are consistent with the second oxidation being a porphyrin ring based oxidation as found in related systems.[23,24]

In cathodic DPP sweeps of a solution 10^{-3} M in $[Fe^{III}(H_2O)(TPPS)]^{3-}$ a feature of small peak current appears at E_p = -1.15 V. In cyclic voltammograms a cathodic wave was observed at $E_p(c)$ = -1.2 V (Figure 1a) and the absence of an oxidative component of the wave indicates that the reduced product is chemically unstable under the conditions of the experiment. Electrochemical reduction of $[Fe^{II}(TPP)]$ (Table II) is known to give low-spin d^7 $[Fe^{I}(TPP)]^-$ with no axial ligands rather than a Fe(II) porphyrin π-anion which is probably the case here as well.[25]

Electrochemical studies on the oxo-bridged dimer $[Fe^{III}(TPPS)]_2O^{8-}$ (**3**) were plagued by slow heterogeneous charge transfer which causes many of its electrode processes to be poorly defined on the CV timescale and by adsorption. For our purposes it is only important to note that reduction of the dimer at pH 7 (0.1 M buffer) leads to reductive cleavage (reaction 3) as shown by the appearance of waves at $E_p(c) = -0.28$ V and $E_p(a) = -0.24$ V for the monomeric $[Fe(H_2O)_n(TPPS)]^{3-/4-}$ couple following a reductive scan.

$$\underset{\mathbf{3}}{[Fe^{III}(TPPS)]_2O^{8-}} + 2e^- + H_2O + 2H^+ \rightarrow 2\underset{\mathbf{6}}{[Fe^{II}(H_2O)_n(TPPS)]^{4-}} \quad (3)$$

The Formation of the Nitrosyl Complex $[Fe^{II}(NO)(TPPS)]^{3-}$ (4) (pH <4). Under mildly acidic conditions (pH <4) free NO is generated in solution containing nitrite due to the disproportionation of nitrous acid.[26,27] Once formed NO can react directly with $[Fe^{III}(H_2O)(TPPS)]^{3-}$ to give the nitrosyl complex **4**.

$$3HNO_2 \rightarrow HNO_3 + 2NO + H_2O \quad (4)$$

$$\underset{\mathbf{2}}{[Fe^{III}(H_2O)(TPPS)]^{3-}} + NO \rightarrow \underset{\mathbf{4}}{[Fe^{II}(NO^+)(TPPS)]^{3-}} + H_2O \quad (5)$$

At pH 3 in a solution containing 10^{-4} M **2** and 0.2 M nitrite, the nitrosyl complex **4** is formed in >95% yield after a 15–20-min incubation period. $[Fe^{II}(NO^+)(TPPS)]^{3-}$ is also generated when a solution containing **2** is saturated with NO as judged by UV/visible spectral changes (Table I). The spectrum of (4) is similar to the spectrum of the species formed by electrochemical oxidation of [Fe(NO)(TPP)] in benzonitrile[9b] (Table I), supporting the assignment of **4** as an oxidized porphyrin nitrosyl analogous to $[Fe(NO)(TPP)]^+$. Solutions of **4** are unstable and readily lose NO regenerating the aquo complex **2**. The loss of NO is greatly assisted by exposure to atmospheric oxygen presumably because NO is removed from the system by oxidation to NO_2.

When a solution containing a mixture of $[Fe^{III}(H_2O)(TPPS)]^{3-}$ and $[Fe^{II}(NO^+)(TPPS)]^{3-}$ saturated with NO is reduced by using an excess of sodium dithionite, a new species, whose spectrum (Table I) is very similar to the spectrum of Fe(NO)(TPP) in benzonitrile,[9b] is generated cleanly. This new species, formed by the reduction of **4**, is the reduced nitrosyl complex $[Fe^{II}(NO^-)(TPPS)]^{4-}$ **5** which can also be generated by the reaction between the iron(II) porphyrin and nitrite (see below). The reduction of **4** to **5** is not facile and requires a large excess of dithionite to occur at a reasonable rate.

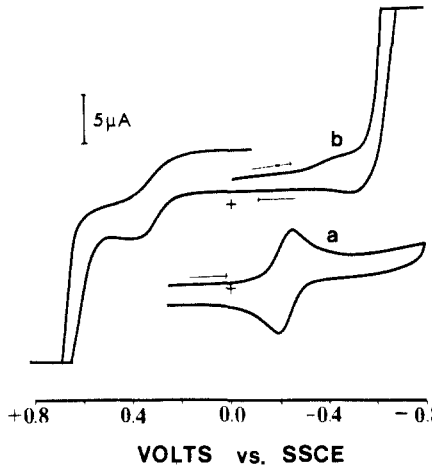

Figure 3. (a) Cyclic voltammogram (100 mV/s vs. SSCE) of 10^{-3} M $[Fe^{III}(H_2O)(TPPS)]^{3-}$ at pH 3.15 in 0.4 M KH_2PO_4 + 0.01 M H_3PO_4 + 0.6 M Na_2SO_4 and (b) with $[NO_2^-] = 10^{-2}$ M. The same result was obtained if scans were begun at 0 V with the initial scan in the positive direction.

For [Fe(NO)(TPP)] some evidence was obtained for the formation of a dinitrosyl complex at high NO pressures.[9] We have obtained no evidence for the formation of a similar species under our conditions, and assume that the mononitrosyl complex is the dominant form in solution.

In the related chemistry of ruthenium ammine complexes, NO undergoes a direct reaction with $Ru(NH_3)_6^{3+}$ to displace an ammine ligand and give the pentaammine nitrosyl complex[28,29] and the reaction between $[Fe^{III}(H_2O)TPPS]^{3-}$ **2** and NO may be an analogous example

$$[Ru^{III}(NH_3)_6]^{3+} + NO \rightarrow [Ru^{II}(NH_3)_5(NO^+)]^{3+} + NH_3 \quad (6)$$

$$[Fe^{III}(H_2O)TPPS]^{3-} + NO \rightarrow [Fe^{II}(NO^+)TPPS]^{3-} + H_2O \quad (7)$$

In the absence of additional information it is unclear as to whether or not the second axial coordination site is occupied by a water molecule to give $[Fe^{II}(N^+O)(H_2O)(TPPS)]^{3-}$, and for convenience we will write the formula of the NO^+ complex as shown in reaction 7. The assignment of oxidation states in nitrosyl complexes has long been a subject of some controversy,[30,31] but in polypyridine complexes of ruthenium and osmium there is clearly a great deal of NO^+ character as shown by chemical and electrochemical studies.[5a,6,32] As noted below, comparisons between the Ru and Os complexes and $[Fe^{II}(NO^+)(TPPS)]^{3-}$ suggest that there is considerable NO^+ character in the bound NO group in **4** as well.

At pH <4, and with intermittent argon purging, nitrite is slowly removed from solution as free NO (reaction 4) as shown by the slow reappearance of the peak for the aqua couple at -0.23 V. Waves for both nitrosyl and aqua couples are typically observed when [nitrite]/[porphyrin] < 2. CV and DPP studies of solutions containing buffer (1 < pH <4) and nitrite at high concentrations (10^{-2} M) with no added porphyrin failed to give an electrochemical response for processes characteristic of either free NO or HONO. At high concentrations of NO added as the gas, a reduction wave is observed at ~-0.7 V.

Electrochemistry of $[Fe^{II}(NO^+)(TPPS)]^{3-}$ (4) (pH < 4). A typical CV of a solution ~10^{-3} M in $[Fe^{III}(H_2O)(TPPS)]^{3-}$ at pH 3.15 and 0.01 M nitrite is shown in Figure 3. In the CV the wave at -0.23 V for the Fe(III)/(II) couple is missing. At +0.7 V the anodic current becomes very large due to the oxidation of

(23) (a) Phillipi, M. A.; Goff, H. M. *J. Am. Chem. Soc.* **1982**, *104*, 6026. (b) Shine, H. J.; Padilla, A. G.; Wu, S. M. *J. Org. Chem.* **1979**, *44*, 4069. (c) Evans, B.; Smith, K. M. *Tetrahedron Lect.* **1977**, *35*, 3079.
(24) Dolphin, D.; Felton, R. H.; Borg, D. C.; Fajer, J. *J. Am. Chem. Soc.* **1970**, *92*, 743.
(25) (a) Hickman, D. L.; Shirazi, A.; Goff, H. M. *Inorg. Chem.* **1985**, *24*, 563. (b) Moshiko, T.; Reed, C. A.; Haller, K. J.; Scheidt, W. R. *Inorg. Chem.* **1984**, *23*, 3192.
(26) Cotton, F. A.; Wilkinson, G. *Advanced Inorganic Chemistry*, 4th ed.; Wiley: New York, 1980; p 430.
(27) Stedman, G. *Adv. Inorg. Chem. Radiochem.* **1979**, *22*, 113.
(28) Armor, J. M.; Scheidegger, H. A.; Taube, H. *J. Am. Chem. Soc.* **1968**, *90*, 5928.
(29) Bottomley, F. *J. Chem. Soc., Dalton Trans.* **1974**, 1600.
(30) Ennemark, J. H.; Feltham, R. D. *Coord. Chem. Rev.* **1974**, *13*, 339.
(31) Bottomley, F. *Coord. Chem. Rev.* **1978**, *26*, 7.
(32) Pipes, D. W.; Meyer, T. J. *Inorg. Chem.* **1984**, *23*, 2466.

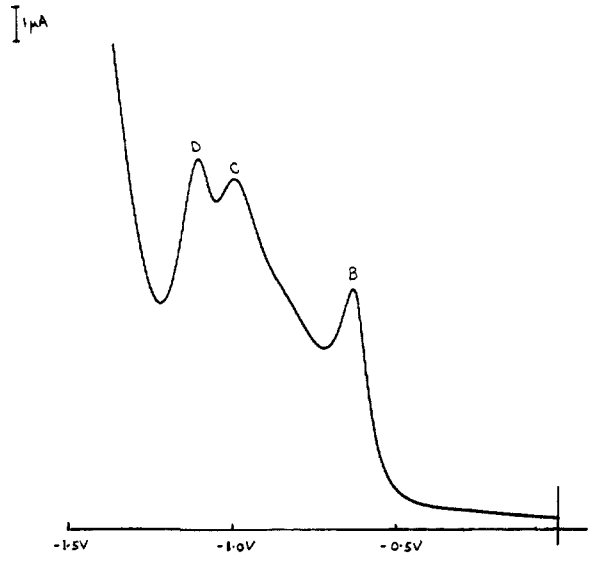

Figure 4. Differential pulse polarogram (10 mV/s) of 3.2×10^{-4} M $[Fe^{III}(H_2O)(TPPS)]^3$ at pH 2.06 (0.1 M in phosphate buffer) vs. SSCE with $[NO_2^-] = 10^{-2}$ M. The second and third reductions of $[Fe^{II}(N^+O)(TPPS)]^{3-}$ occur at peaks B and C, and peak D corresponds to the $[Fe^{II}(H_2O)_n(TPPS)]^{4-}/[Fe^{I}(TPPS)]^{5-}$ couple.

excess nitrite. Past ~-0.5 V the onset of a catalytic wave due to reduciton of nitrite occurs. A wave is also observed at ~+0.35 V which is poorly defined suggesting that the electrode process involved has poor charge-transfer characteristics. In the DPP scan in Figure 4 a reductive process (B) is observed at about -0.6 V as a well-defined, pH-dependent peak suggesting that a rapid reduction occurs at this potential. By contrast the wave at +0.35 V appears as a peak of very low peak current confirming its slow charge-transfer characteristics.

When a CV sweep is started at 0.0 V, a noticeable current flow was observed when the circuit was connected. Initiation of sweeps at +0.4 V gave no evidence for a prompt current flow. These and related observations suggest that the species in bulk solution is reduced at potentials more negative than +0.35 V but is stable toward reduction at more positive potentials. From these observations we conclude that the species in solution is the oxidized form of the nitrosyl complex **4** and that the process at +0.35 V is the 1-electron reduction of **4** to give **5**,

$$[Fe^{II}(NO^+)(TPPS)]^{3-} + e^- \rightarrow [Fe^{II}(NO\cdot)(TPPS)]^{4-} \quad (8)$$
4 **5**

which is followed by a second, 1-electron reduction (B) to give $[Fe^{II}(NO^-)(TPPS)]^{5-}$ (**7**),

$$[Fe^{II}(NO\cdot)(TPPS)]^{4-} + e^- \rightarrow [Fe^{II}(NO^-)(TPPS)]^{5-}$$
5 **7**

$$E_{1/2} = -0.64 \text{ V at pH } > 2.6 \quad (9)$$

As noted below, and in the Discussion, the second reduction (reaction 9) is proton-dependent at pH <2.6 (Figure 5).

UV/visible spectroscopic examination of solutions containing moderate excesses of nitrite and Fe(III) porphyrin, 3 < [nitrite]/[porphyrin] < 20, showed that the dominant species in solution is the aqua complex $[Fe^{III}(H_2O)(TPPS)]^{3-}$. Under these conditions the formation of the nitrosyl complex **4** by reaction 7 is much slower than in 0.1 M nitrite. Even though the aqua complex is the dominant form in solution, cyclic voltammetry showed no evidence for the wave at -0.23 V for the $[Fe(H_2O)(TPPS)]^{3-/4-}$ couple, only the characteristic waves of the nitrosyl couples were observed, and the formation of the nitrosyl complex must be catalyzed during the electrochemical process under these conditions.[33]

(33) One possible origin for catalyzed nitrosyl formation is that upon approaching the electrode the aqua complex encounters a high local concentration of chemisorbed NO and is converted into the nitrosyl complex.

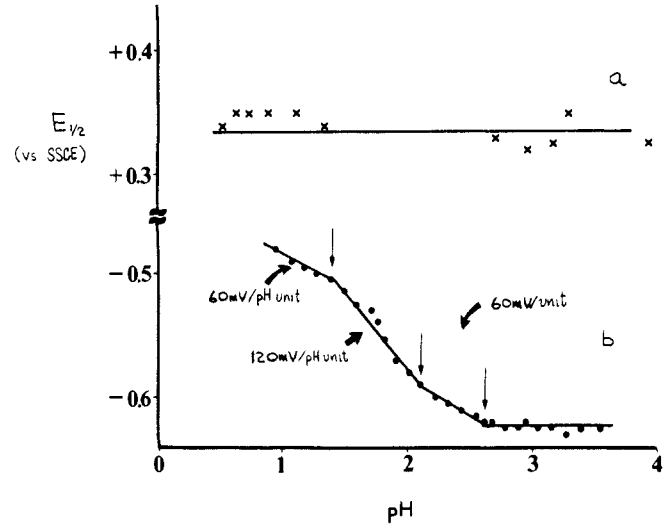

Figure 5. pH dependences vs. SSCE for the first two reductions of $[Fe^{II}(NO^+)(TPPS)]^{3-}$. The data were obtained at an activated carbon electrode in solutions 2×10^{-3} M in $[Fe^{III}(H_2O)(TPPS)]^{3-}$, 2×10^{-2} M in NO_2^-, and 0.6 M in H_2SO_4. For the $Fe^{II}(NO\cdot)/Fe^{II}(NO^-)$ wave, the phosphate buffer used above pH 2.9 caused an increase in $E_{1/2}$ by ~40 mV compared to the HSO_4^- buffer used below pH 2.9 The data in phosphate have been corrected by subtracting 40 mV.

If solutions of buffer and 0.6 M Na_2SO_4 are used, the pH dependences of the two nitrosyl-based reduction waves were studied by using DPP with an activated carbon electrode under conditions where nitrite was in 5-10-fold excess (Figure 5). The first reduction of the nitrosyl complex, reaction 8, is pH-independent in the range 0.5 < pH <3.5, but the second reduction, reaction 9, has a complex pH dependence. Related behavior has been observed for nitrosyl-polypyridine complexes of ruthenium and osmium.[6]

Further reductive processes were studied by DPP, using activated carbon electrodes, Figure 4. The peak labeled D was only observed when pH <3.5 and then only with low added nitrite, [nitrite]/[porphyrin] < 3. The peak is pH-independent and not enhanced by the addition of added nitrite. From these observations and the observed potential (-1.12 V), the wave appears to arise from the $[Fe^{II}(H_2O)(TPPS)]^{4-}/[Fe^{I}(TPPS)]^{5-}$ couple. In contrast, the peak labeled C is increased substantially with the addition of more nitrite and generally obscures process D completely at [nitrite]/[porphyrin] > 3. Reduction C at $E_{1/2} = -0.99$ V appears to be a further reduction of the nitrosyl complex. It is pH-independent at pH <3.5.

Formation and Electrochemistry of the Nitrosyl Complexes at pH >4. At low nitrite concentrations and pH >3.5, $[Fe^{III}(H_2O)(TPPS)]^{3-}$ is the dominant species in solution as judged by both UV/visible spectroscopy and CV and DPP scans. Cyclic voltammograms (Figure 3) show a wave for the reductive component of the $[Fe(H_2O)(TPPS)]^{3-/4-}$ couple at $E_p(c) = -0.26$ V but with a diminished (often undetectable) return wave at $E_p(a) = -0.20$ V. In addition, a wave corresponding to the second reduction at the nitrosyl ligand (reaction 9) occurs at $E_p(c) = -0.75$ V (phosphate buffer and no added Na_2SO_4) as do the oxidative and reductive components for the first nitrosyl reduction at $E_{1/2} = +0.32$ V.

The CV experiment shows that a second path exists for the formation of the nitrosyl complexes based on metal-centered Fe(III) → Fe(II) reduction followed by nitrosation

$$[Fe^{III}(H_2O)TPPS]^{3-} + e^- \rightarrow [Fe^{II}(H_2O)TPPS]^{4-} \quad (10)$$
2 **6**

$$[Fe^{II}(H_2O)TPPS]^{4-} + HONO + H^+ \rightarrow$$
6

$$[Fe^{II}(NO^+)(TPPS)]^{3-} + H_2O \quad (11)$$
5

and reduction according to reaction 8. Evidence for this chemistry was obtained directly from spectroscopic studies on porphyrin-

Table III. Reduction Products of the $[Fe^{III}(H_2O)(TPPS)]^{3-}$ Catalyzed Electroreduction of NO_2^- at -0.9 V at a 12-cm^2 Hg Pool

	$[Fe^{III}]^a$	$[NO_2^-]^{b,c}/[Fe^{III}]$	electrons added per NO_2^-	electrolysis time, h	current, mA init	current, mA final	product[d] current efficiency, % NH_3	NH_2OH^e	N_2O	N_2
				pH 4.5[f]						
1.	3×10^{-5} M	333	4.0	4	~80	2.4	49	41	9	<1
2.	7.5×10^{-5} M	133	3.44	2	~80	6.6	45	37	18	<1
3.	1.2×10^{-6} M, <1%	8300	3.59	4	58	2.0	26	63	11	
4.	2.5×10^{-4} M	40	5.18	$7^1/_2$	100	0.16	97	0	3	<1
5.	blank[g]		1.3	$4^1/_2$	15	2.7	22	19	59	<1
				pH 6.7						
6.	2.4×10^{-4} M	82[h]	2.94[i]	8	18	5.8	82	11	7	<1
7.	2.5×10^{-4} M	40	5.25	21.5	6.8	1.2	95	0	5	<1
8.	1.0×10^{-3} M	20	5.42	23	13	0.08	97	0	3	<1
				hydroxylamine; pH 4.5						
9.	3.0×10^{-4} M	67[h]	1.81	4.5	13	0.08	~100[j]			

[a] $[Fe^{III}(H_2O)(TPPS)^{3-}]$. [b] $[NO_2^-]/[Fe^{III}(H_2O)(TPPS)^{3-}]$. [c] Initially $[NO_2^-] = 0.01$ M unless otherwise indicated. [d] Current efficiencies calculated from product analyses and electrochemical stoichiometries, e.g., $NO_2 + 6e^- + 7H^+ \rightarrow NH_3 + 2H_2O$. [e] Current efficiency for NH_2OH is assumed to be 100 - (%NH_3 + %N_2O). [f] 0.5 M KH_2PO_4. [g] Blank using a freshly cleaned vycor divider. If the vycor divider is not freshly cleaned, sufficient catalyst leaches from the glass to cause catalyzed reduction of nitrite as shown by enhanced currents and colorimetric detection of NH_2OH. [h] $[NO_2^-] = 0.02$ M. [i] Electrolysis only allowed to proceed until ~50% of the nitrite had been reduced to products. [j] Some N_2O (~6%) appeared during the reaction due to the disproportionation of NH_2OH.

containing solutions. Addition of about 20 equiv of sodium dithionite (or 10 equiv of Cr^{2+} at pH >3.5) to a 2×10^{-4} M solution of **2** cleanly generated the Fe(II) porphyrin **6** with an intense Soret band at 424 nm (Table I). The Fe(II) complex is very air-sensitive as expected[34] and demetallates rapidly at pH <3.5, which is also known for water-soluble M(II) porphyrins in strongly acidic media.[35,36] Demetalation of the Fe(II) porphyrin gives a green species having a spectrum similar to that of the diprotonated porphyrin (for H_4TPPS^{2-}, λ_{max} = 438, 645 nm[37] and a product with λ_{max} = 488, 708 nm which appears to be an aggregation product of H_4TPPS^{2-}. Demetalation of the Fe(II) porphyrin at pH <5 appears to be the major source of deactivation of the catalyst in the NO_2^- reduction studies described below.

Addition of 20 equiv of nitrite to solutions of **6** at pH 7 (dithionite reduction) gave $[Fe^{II}(NO^{\bullet})TPPS]^{3-}$ cleanly. The existence of a bound nitrosyl/nitrite equilibria is well-known for poly(pyridine) complexes of ruthenium and osmium,[3b,7,32] e.g.,

$$[(bpy)_2(py)Ru^{II}(NO_2)]^+ + 2H^+ \rightarrow [(bpy)_2(py)Ru^{II}(NO)]^{3+} + H_2O \quad (12)$$

For the iron porphyrin complex the relevant equilibrium is

$$[Fe^{II}(H_2O)_n(TPPS)]^{4-} + 2H^+ + NO_2^- \rightarrow [Fe^{II}(NO^+)(TPPS)]^{3-} + nH_2O \quad (13)$$

There is no direct evidence for prior coordination of the nitrite ligand before formation of the nitrosyl, but from our observations it is clear that for the equilibrium in reaction 13, $K >> 1$ at pH 3.5. Once again, it is unknown whether or not a second water molecule occupies the second axial position. The same spectral observations were made even out to pH 6.48 where the second nitrosyl reduction is finally lost in the CV. From these observations we conclude that $K > 2 \times 10^{14}$ for reaction 13 as written and that the Fe^{II}-NO^+ rather than the Fe^{II}-NO_2^- complex persists even under these nearly neutral conditions.

Under conditions where the oxo-bridged dimer is the predominant species in solution, formation of the nitrosyl complexes occurs via reaction 11 after the dimer is reduced to Fe(II) at potentials more negative than -0.3 V, as shown by the appearance of the expected nitrosyl waves following a reductive scan past -0.3 V.

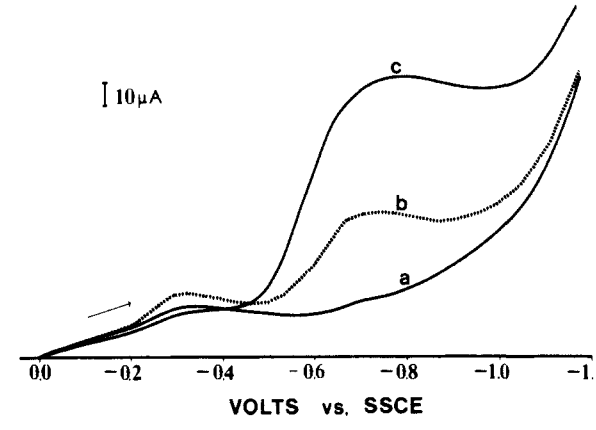

Figure 6. Linear sweep voltammograms (50 mV/s) for 1.4×10^{-3} M $[Fe^{III}(H_2O)(TPPS)]^{3-}$ and 5×10^{-3} M NO_2^-: (a) pH 4.07; (b) pH 3.35; (c) pH 2.6-2.9.

Catalysis. Properties of the Electrocatalytic Waves. In cyclic voltammograms of solutions containing both nitrite and porphyrin, reductions beyond the $[Fe^{II}(NO)(TPPS)]^{4-/5-}$ stage are concealed in a broad multielectron envelope. As found earlier for nitrosyl polypyridine complexes of ruthenium and osmium,[6] the characteristics of the further reductive processes based on the iron porphyrin are highly pH-dependent (Figure 6).

At pH 4.0 a reductive scan past the $Fe^{II}(NO^{\bullet})/Fe^{II}(NO^-)$ wave gives a broad featureless bump suggesting that kinetically slow processes are occurring. A small return wave (at ~-0.5 V) for the $Fe^{II}(NO^-) \rightarrow Fe^{II}(NO^{\bullet})$ couple appears on the oxidative return sweep showing that reduction past the $Fe^{II}(NO^{\bullet})$ stage is slow at the electrode at pH 4. At pH 3.35, a dramatic enhancement of the catalytic current occurs (Figure 6) and the peak potential of the broad wave shifts oxidatively. Both observations are consistent with the presence of proton-dependent reductions. The catalytic wave grows rapidly between pH 4 and 3 but by pH 2.9 the current enhancement becomes saturated with little or no increase observed in the range 2.6 < pH <2.9. Comparing the area under the catalytic wave with the corresponding area under the 1-electron wave for the $[Fe(H_2O)TPPS]^{3-/4-}$ couple before the addition of nitrite demonstrates that the catalytic wave is multi-electron in character.

By pH 3.0 scanning negatively through the multielectron wave and then oxidatively gives waves for only the $Fe^{II}(NO^{\bullet})/Fe^{II}(NO^-)$ and $Fe^{II}(NO^+)/Fe^{II}(NO^{\bullet})$ couples. Under these conditions, reduction, loss of the reduced ligand, and reformation of $[Fe^{II}(NO^+)(TPPS)]^{3-}$ are all rapid on the CV time scale.

Products of the Catalytic Reductions. The conditions used for the bulk electrocatalytic experiments and the products derived

(34) Espenson, J. H.; Christenson, R. J. *Inorg. Chem.* **1977**, *16*, 256.
(35) Reynolds, W. L.; Kooda, K.; Florine, B.; Johnson, N.; Thielman, K. *Int. J. Chem. Kinet.* **1980**, *12*, 97.
(36) Reynolds, W. L.; Schufman, J.; Chan, F.; Brasted, R. C., Jr. *Int. J. Chem. Kinet.* **1977**, *9*, 777.
(37) Geibel, J.; Chang, C. K.; Traylor, T. G. *J. Am. Chem. Soc.* **1975**, *97*, 5924.
(38) Meyer, T. J.; Godwin, J. B.; Winterton, N. *J. Chem. Soc. D* **1970**, 872.

from the reductions are shown in Table III. Although similar results were obtained at vitreous carbon or Hg electrodes, most of the quantitative work was carried out at Hg because of higher current, densities, fewer complications from electrode fouling, and the known electrode area. Controlled-potential electrolyses were carried out at -0.9 V which is well into the catalytic envelope. Electrolysis at lower potentials, for example, to the 2-electron stage to give $Fe^{II}(NO^-)$ at ~-0.55 V (pH 4.5) changes the product distribution and favors N_2O and hydroxylamine at the expense of ammonia.[39] However, our major concern here was in the production of NH_3, and the majority of electrolyses were carried out at -0.9 V. Linear sweep voltammetry at a carbon disk electrode shows negligible reducing current for nitrite alone, even out to -1.0 V at pH 4.5 and even lower background currents at pH 7. A blank electrocatalytic run at pH 4.5 in the absence of the porphyrin catalyst had an initial current of 15 mA which died off rapidly, with between 1 and 1.5 electrons per molecule of available nitrite having been passed. At the end of the electrolysis period, addition of further NO_2^- caused no current increase suggesting that the reduction had affected the Hg electrode inhibiting further reduction. The reduction products of the noncatalyzed reduction were mainly N_2O along with a small proportion of ammonia and presumably hydroxylamine (experiment 5, Table III). With added porphyrin the level of catalytic current increased dramatically and the product distribution was altered in favor of the more highly reduced products.

In experiment 7 in Table III it was found that the catalyst was >86% intact after ~36 turnovers at pH 6.7. In addition, the large turnover numbers at pH 4.5 suggest that degradation of the catalyst by demetalation of the Fe(II) porphyrin is relatively slow at pH 4.5 as well.

Under nearly neutral conditions (pH 6.7) the catalyst is present initially largely as the μ-oxo dimer **3** until reduction to Fe(II) occurs. The electrolyses at pH 6.7 are characterized by low currents and the formation of ammonia as the major product. Hydroxylamine appears to be an intermediate in the reduction which builds up in the solution to a limited extent and is subsequently reduced to ammonia. From the data in Table III, if a run was stopped before completion with catalytic currents maintained at 5 mA, hydroxylamine appears to exist in the solutions as shown by experiment 6. In contrast, if the catalytic run was allowed to proceed to completion, e.g., experiments 7 and 8 in Table III, ammonia is obtained in >95% current efficiency. In the blank experiment involving added hydroxylammine (experiment 9 in Table III) the catalytic current was ~60% that for NO_2^- at the same concentration and NH_3 was the reduced product.

At pH 6.7 the catalytic currents are low and increase roughly linearly with added porphyrin and nitrite. The dependence on nitrite suggests that at pH 6.7, the rate-limiting step in the catalytic reduction may be the formation of the $Fe^{II}(NO^+)$ complex.

At pH 4.5-5, the catalyst is largely present as the Fe(III) aqua complex **2** before reduction. Catalytic currents are considerably enhanced compared to pH 6.7 and CV experiments suggest that a roughly linear dependence exists between the magnitude of the catalytic current and the concentration of the added porphyrin. However, at the high current densities of the electrolyses, the initial catalytic currents are relatively insensitive to porphyrin concentration (Table III) and it is conceivable that the majority of the catalysis is taking place near or at adsorbed sites at the electrode surface.

Current densities of 6.4 mA/cm^2 were obtained at pH 4.5 at a catalyst concentration of 7.5×10^{-5} M. At a catalyst concentration of 1.5×10^{-6} M, initial current densities of 4.6 mA/cm^2 were obtained, and under these conditions 58% of the nitrite was apparently converted into hydroxylamine with over 4800 turnovers (experiment 3 Table III). In this pH range, hydroxylamine appears to build up in solution to a significant degree and further reduction to ammonia occurs readily (Table III) but at a relatively reduced rate compared to the reduction of nitrite to hydroxylamine (compare experiments 9 and 4). In all these experiments N_2O was an important side product and its possible origin will be discussed below. Runs using low porphyrin concentrations and the short times associated with incomplete electrolysis tended to favor the formation of N_2O. Runs at low porphyrin concentrations, and high turnover numbers, tended to favor hydroxylamine at the expense of ammonia (compare experiments 3 and 1).

The problems encountered in analyzing for hydroxylamine were documented earlier. Under the conditions of the experiments listed in Table III, ^{14}N NMR analysis for NH_3OH^+ at pH 3.8 was relatively insensitive even at a concentration level of 5×10^{-3} M solution, which is the expected concentration level expected of a product generated from 50% reduction of nitrite to hydroxylamine in most of the experiments listed in Table III. An added complication is that NH_3OH^+ is unstable in solution in the presence of the porphyrin via a number of side reactions. Solutions containing both nitrite and hydroxylamine are unstable with respect to N_2O under our conditions. A solution containing 0.1 M NO_2^- + 0.1 M NH_3OH^+ at pH 4 gave N_2O with the reaction nearly complete in ~20 min. In more dilute solutions the reaction is slower, but even at 0.01 M NO_2^- + 0.01 M NH_3OH^+, considerable amounts of N_2O were obtained after 12 h as detected by GC and the absence of ^{14}N resonances for NO_2^- or NH_3OH^+ in the ^{14}N NMR spectrum of the solution. In fact, the main evidence for formation of NH_3OH^+ as a product was by the colorimetric test described earlier in which a small amount of porphyrin was used as catalyst and up to 70% of the nitrite was converted to hydroxylamine. The combination of competing reactions and our inability to develop an adequate procedure for NH_3OH^+ means that some, if not all, of the data on product distributions in Table III may not be a simple reflection of catalytic NO_2^- reduction. However, it seems clear that NH_3OH^+ is an intermediate and NH_4^+ the final product. We have no clear insight into how much of the N_2O formed at -0.9 V may have come from decomposition of NH_3OH^+.

In most of the runs, the amount of dinitrogen in the dead space above the solution was measured before and after the catalytic run by GC. In all cases there was a slight increase in the amount of dinitrogen. However, the amount observed accounted for <1% of products and <1% of the current efficiency, and even the small amount observed may have its origin in slow diffusion of air into the cell over the rather extended times of the electrolyses.

Volume changes were measured for most of the catalytic runs. Increases in volume were generally slightly smaller than, but consistent with, the amount of N_2O determined by GC.

Mixing experiments conducted in the presence of the porphyrin showed that insignificant amounts of NH_3OH^+ formed from a mixture of nitrite and ammonia (0.1 M) at pH 4.5. However, solutions containing only hydroxylamine and porphyrin at pH 4.5 did generate some N_2O apparently by porphyrin-catalyzed disproportionation of NH_3OH^+ into NH_4^+ and N_2O.

Discussion

Mechanism of the Catalytic Reduction. Detailed electrochemical studies on the reduction of the coordinated nitrosyl ligand to ammine in polypyridine complexes of ruthenium and osmium have led to mechanisms based on a series of 1-electron steps. In specific detail, the mechanism proposed for reduction of $[Os^{II}(NO)(tpy)(bpy)]^{3+}$ (tpy is 2,2′,2″-terpyridine; bpy is 2,2′-bipyridine) involves a series of successive intermediates of the type $[Os^{II}(NO)(tpy)(bpy)]^{2+}$, $[Os(NO)(tpy)(bpy)]^{+}$, $[Os(NHO)(tpy)(bpy)]^{2+}$, $[Os^{V}(N)(tpy)(bpy)]^{2+}$ or $[Os(NH_2O)(tpy)(bpy)]^{2+}$, $[Os^{IV}(=NH)(tpy)(bpy)]^{2+}$, and $[Os(NH_3)(tpy)(bpy)]^{3+}$. A key step in the reduction is the initial formation of the nitrosyl complex by an initial acid/base step, reaction 12.[6,32,38] In the nitrosyl complex there are low-lying levels, largely $\pi^*(NO)$ in character, which provide a basis for the addition of electrons and for the initiation of the series of 1-electron events which finally lead to coordinated ammonia.

The chemistry of the iron porphyrin system parallels that of the ruthenium and osmium complexes in many respects, and it is of value to compare the various steps involved among the different types of systems.

(39) Rhodes, M.; Barley, M. H.; Meyer, T. J., work in progress.

Formation of the Nitrosyl. In the ruthenium and osmium complexes nitrite ion is firmly bound and the acid/base chemistry occurs within the coordination sphere as shown in reaction 12.

Under our conditions in aqueous solution at moderate nitrite concentrations, we find no spectral or electrochemical evidence for the binding of nitrite to either the Fe(II) or Fe(III) porphyrins. The low affinity for NO_2^- in competition with water molecules for the axial sites is probably a consequence of the enhanced solvation energy of the anion in water compared at least to nonaqueous solvents, electrostatic effects, and a lowered electronic interaction with the, probably, spin free metal ion. The importance of solvation energy stabilization of the free anion can be seen by comparisons with data in nonaqueous solvents where, for example, in dichloromethane or THF even weakly binding anions like ClO_4^- bind to the metal center in $[Fe^{III}(TPP)]^+$ with a relatively high affinity.[40]

Nitrosyl–iron porphyrin complexes are generated in solution by adding NO to $[Fe^{III}(H_2O)(TPPS)]^{3-}$ (reaction 7) or by prior reduction to Fe(II) in the presence of NO_2^- (reaction 11 followed by reaction 8). The latter reaction occurs even at pH 6.7, suggesting a high thermodynamic stability for the nitrosyl complex. The complex is kinetically unstable in air because of loss of NO followed by irreversible oxidation to NO_2. Electrochemical generation necessarily gives the reduced form $[Fe^{II}(NO)(TPPS)]^{4-}$ because the Fe(III)/(II) reduction occurs at a potential more negative ($E_{1/2}$ = −0.23 V) than the potential for the $Fe^{II}(NO^+) \rightarrow Fe^{II}(NO)$ reduction at ~+0.35 V. In the presence of NO_2^-, the μ-oxo dimer $[[Fe^{III}TPPS]_2O]^{8-}$ is also reduced to $[Fe^{II}(NO)(TPPS)]^{4-}$.

The First Reduction. The reduction $[Fe^{II}(NO^+)(TPPS)]^{3-} + e^- \rightarrow [Fe^{II}(NO^{\cdot})(TPPS)]^{4-}$ is pH-independent and from both the wave-shape- and scan-rate-dependence studies is kinetically slow at the electrode. The second reduction at the nitrosyl ligand bound to polypyridine complexes of ruthenium and osmium is also kinetically slow and in the work it was suggested that either a slow isomerization might be occurring between a linear and a bent form of the nitrosyl ligand or perhaps that reduction is accompanied by a decrease in coordination number from 6 to 5. In any case, the first reduction appears to involve addition of an electron to a level largely $\pi^*(NO)$ in character for all three types of complexes perhaps complicated by either an isomerization, $Fe^{II}(NO^{\cdot}) \rightarrow Fe^{III}(NO^-)$, or a change in coordination number for the iron porphyrin.

The Second Reduction. In the net sense the second reduction is probably also NO based, either

$$[Fe^{II}(NO^{\cdot})(TPPS)]^{4-} + e^- \rightarrow [Fe^{II}(NO^-)(TPPS)]^{5-} \quad (14)$$

or perhaps

$$[Fe^{III}(NO^-)(TPPS)]^{4-} + e^- \rightarrow [Fe^{II}(NO^-)(TPPS)]^{5-}$$
$$\mathbf{5} \qquad\qquad\qquad\qquad \mathbf{7}$$

At pH >2.6 the second reduction is also pH-independent. However, below pH 2.6 the second reduction assumes a pH dependence. The proton stoichiometries shown in reactions 4–6 were deduced from the results of pH-dependent $E_{1/2}$ measurements.

$$2.6>pH>2.1: \quad [Fe^{II}(NO^{\cdot})(TPPS)]^{4-} + e^- + H^+ \rightarrow [Fe^{II}(NHO)TPPS]^{4-} \quad (15)$$

$$2.1>pH>1.4: \quad [Fe^{II}(NO^{\cdot})TPPS]^{4-} + e^- + 2H^+ \rightarrow [Fe^{II}(NH_2O^+)TPPS]^{3-} \text{ (or } [Fe^{VI}(\equiv N)(TPPS)]^{3-}) \quad (16)$$

$$pH<1.4: \quad [Fe^{II}(NHO^{\cdot+})TPPS]^{3-} + e^- + H^+ \rightarrow [Fe^{II}(NH_2O^+)TPPS]^{3-} \text{ (or } [Fe^{VI}(\equiv N)(TPPS)]^{3-}) \quad (17)$$

The absence of a proton dependence for the parent Fe(III)/Fe(II) couple, $[Fe(H_2O)_n(TPPS)]^{3-/4-}$ (n = 1 or 2), suggests that protonation is not occurring at the sulfonate sites of the TPPS ligand and, instead, is confined to the nitrosyl ligand.

The results of the proton-dependent $E_{1/2}$ studies give insight into proton and electron content but not on electronic or molecular structure, hence the uncertainty in the assignments of the products in reactions 15–17. Procedence for protonation of a bent, doubly reduced, nitrosyl ligand at the nitrogen atom does exist for at least one case based on an osmium nitrosyl as shown by an X-ray crystallographic study.[41] Protonation of $[Fe^{II}(NO^{\cdot})TPPS]^{4-}$ prior to reduction in strongly acidic solution could occur at either the N or O atoms.

As written, the reduced product in reaction 16 is either $[Fe^{II}(NH_2O^+)TPPS]^{3-}$, a protonated form of $[Fe^{II}(NHO)(TPPS)]^{4-}$, or, perhaps, by dehydration the Fe(VI)-nitrido complex ($[Fe^{II}(N^+)TPPS]^{3-} \leftrightarrow [Fe^{VI}(\equiv N)(TPPS)]^{3-}$). Stable porphyrin nitrido complexes of Os(VI) are known, e.g., $[Os^{VI}(\equiv N)(DEP)OMe]$.[42] Another alternative is that the intermediate is $[Fe^{IV}(NHOH^-)TPPS]^{3-}$ in which oxidation state IV is stabilized by π-electron donation from the deprotonated hydroxylamine ligand, $[(OH)HN:]^-$. Depending upon the state of hydration, a number of reasonable formulations are possible for the twice-protonated intermediate and in the absence of further experimental evidence its exact formulation remains obscure.

The Third Reduction. The catalytic experiments were carried out above pH 2.6 where the twice-reduced intermediate is $[Fe^{I}(NO^-)(TPPS)]^{5-}$. Further reduction leads to the catalytic production of NH_4^+ or NH_3OH^+ via a process or processes that are strongly acid-catalyzed and which obscure any further reductive processes. For polypyridine complexes of Ru and Os there is a clearly defined third stage which involves the addition of an electron to give in the limiting net sense, either $[(tpy)(bpy)M^{II}(NH_2O^{\cdot})]^{2+}$ or the dehydrated form $[(tpy)(bpy)M^{V}(N)]^{2+}$).[6] Recall that there is evidence from the results of DPP experiments (Figure 4) for a third reduction of the porphyrin at pH 2.06. If the porphyrin reaches a 3-electron-reduced intermediate, the appearance of hydroxylamine as a product could occur through the addition of two electrons and a proton in acidic solution,

$$[Fe^{II}(NH_2O^+)TPPS]^{3-} + 2e^- + H^+ \rightarrow [Fe^{II}(NH_2OH)TPPS]^{4-}$$

or by the addition of two electrons and a proton to a Fe(VI) nitrido intermediate to give $Fe^{IV}{=}NH$,

$$[Fe^{VI}(\equiv N)(TPPS)]^{3-} + 2e^- + H^+ \rightarrow [Fe^{IV}(=NH)(TPPS)]^{4-}$$

followed by hydration at the ligand and intramolecular reduction of the metal

$$[Fe^{IV}(=NH)(TPPS)]^{4-} + H_2O \rightarrow [Fe^{II}(NH_2OH)TPPS]^{4-}$$

The latter reaction has been reported to occur for $[(tpy)(bpy)Ru^{IV}{=}NH]^{2+}$ with a half-time of ~100 s in H_2O at room temperature.[43] The existence of $Fe^{IV}{=}NH$ even as an unobservable kinetic intermediate is also appealing in providing a possible basis for the further reduction of NH_2OH to NH_3 via

$$[Fe^{II}(NH_2OH)(TPPS)]^{4-} \rightleftharpoons [Fe^{IV}(=NH)(TPPS)]^{4-} + H_2O$$

$$[Fe^{IV}(=NH)(TPPS)]^{4-} + 2H^+ + 2e^- \rightarrow [Fe^{II}(NH_3)(TPPS)]^{4-}$$

The Reduction Products. From the results obtained in the catalytic runs, ammonia is the ultimate product, but at pH ~5 hydroxylamine apparently builds up to a more substantial degree than at pH 6.7. The buildup at pH 4.5 is consistent with the fact that the rate of reduction of nitrite to hydroxylamine is noticeably faster than the rate of reduction of hydroxylamine to NH_3 as evidenced by comparative catalytic currents. At pH 6.7, the two rates are more nearly comparable, reduction of nitrite is only about 60% faster than reduction of NH_2OH, and hydroxylamine competes with nitrite for the catalyst on a more even basis.

(40) Scheidt, W. R.; Reed, C. A. *J. Am. Chem. Soc.* **1978**, *100*, 666.

(41) Wilson, R. D.; Ibers, J. A. *Inorg. Chem.* **1979**, *18*, 336.

(42) Buchler, J. W.; Kokisch, W.; Smith, P. D. *Struct. Bonding (Berlin)* **1978**, *34*, 1.

(43) Thompson, M. S.; Meyer, T. J. *J. Am. Chem. Soc.* **1981**, *103*, 5577.

Scheme I

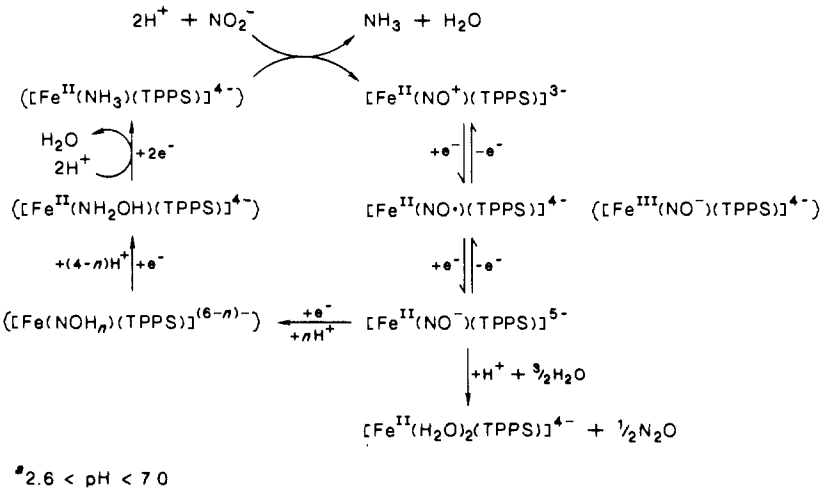

The pK_a for NH_3OH^+ is 6.03.[44] One explanation for the buildup of hydroxylamine at pH 4.5 is that a competition exists between protonation-induced dissociation of the ligand

$$[Fe^{II}(NH_2OH)(TPPS)]^{4-} + H^+ + 2H_2O \rightarrow [Fe^{II}(H_2O)_2TPPS]^{4-} + NH_3OH^+$$

and further reduction,

$$[Fe^{II}(NH_2OH)TPPS]^{4-} + 2e^- + 2H^+ \rightarrow [Fe^{II}(NH_3)TPPS]^{4-} + H_2O$$

At both pH 4.5 and 6.7, the final step in the catalytic cycle is the loss of NH_3 or NH_2OH,

$$[Fe^{II}(L)TPPS]^{4-} + H^+ + 2H_2O \rightarrow [Fe^{II}(H_2O)_2TPPS]^{4-} + HL^+ \quad L = NH_3, NH_2OH \quad (18)$$

and reformation of the nitrosyl complex,

$$[Fe^{II}(H_2O)_2TPPS]^{4-} + 2H^+ + NO_2^- + e^- \rightarrow [Fe^{II}(NO\cdot)TPPS]^{4-} + 3H_2O \quad (19)$$

The loss of reduced ligand is a crucial step in the overall catalytic cycle and, given the axial lability of the iron porphyrin, distinguishes the catalytic system from the ruthenium and osmium complexes where the reduction is stoichiometric. The net axial exchange of NO^+ for NH_3 is rapid in acidic solution. At pH 3.95, the return oxidative scan after scanning through the reductive catalytic region to −1.0 V at a scan rate of 100 mV per gave only waves associated with the nitrosyl couples, showing that exchange of NO^+ for NH_3 is complete on that time scale.

Mechanism of Catalysis. Enough information appears to be available concerning the mechanism of nitrite reduction by the iron porphyrin to suggest the overall pattern of reactions in Scheme I. As noted above, intermediates past those that appear in Scheme I, analogous to those observed in the reductions based on polypyridyl complexes of Ru and Os, may also appear, but we have no experimental evidence for their intervention. In Scheme I, intermediates whose presence has been inferred without experimental evidence or represent alternate formulations are shown by the braces.

The fact that no more than trace amounts of N_2 and N_2H_4 were found among the products is significant. It clearly suggests that possible coupling reactions involving intermediates of the type $[Fe^V(\equiv N)(TPPS)]^{4-}$ or $[Fe^{IV}(=NH)(TPPS)]^{4-}$, if they are present, are not important competing steps to further reduction and completion of the catalytic cycle.

The consistent appearance of N_2O as a product could be from several origins, and reductive coupling appears to be one of them. Controlled-potential electrolysis at the 2-electron stage for $[M(NO)(tpy)(bpy)]^{3+}$ (M = Ru, Os) clearly gives N_2O as a major product.[39] Catalytic reduction of NO_2^- by the soluble porphyrin at the 2-electron stage (−0.55 V) leads to a considerable increase in the yield of N_2O. The appearance of N_2O at the 2-electron stage is an expected result, at least given the implied demands of the reaction. The mechanism could involve an initial coupling via hyponitrite ($N_2O_2^{2-}$) bridge formation,

$$2[Fe^{II}(NO^-)(TPPS)]^{5-} \rightarrow [(TPPS)Fe^{II}(N_2O_2)Fe^{II}(TPPS)]^{10-}$$

followed by N_2O formation,

$$[(TPPS)Fe^{II}(N_2O_2)Fe^{II}(TPPS)]^{10-} + 2H^+ + H_2O \rightarrow N_2O + 2[Fe^{II}(H_2O)(TPPS)]^{4-}$$

or protonation,

$$[Fe^{II}(NO^-)(TPPS)]^{5-} + H^+ \rightarrow [Fe^{II}(NHO)(TPPS)]^{4-}$$

followed by coupling,

$$H_2O + 2[Fe^{II}(NHO)(TPPS)]^{4-} \rightarrow N_2O + 2[Fe^{II}(H_2O)(TPPS)]^{4-}$$

The appearance of the N-N coupling chemistry at the $2e^-$ stage but not at the $3e^-$ (N_2) or $5e^-$ (N_2H_4) stages is clearly of interest and is under further investigation.

Reduction Products. Comparisons with Other Systems. The noncatalytic electroreduction of nitrite at various potentials gives a high proportion of hydroxylamine as product. As an example, reduction of HONO at a Pt electrode in 0.1 M $HClO_4$ at −0.22 V gives NH_3OH^+ with a current efficiency of approximately 64%,[45] and electroreduction at mercury at −1.1 V at pH 3 gives NH_3OH^+ with a current efficiency of 45%.[46] It is interesting to note that hydroxylamine is produced commercially by the electrolytic reduction of nitrite.[47] It is conceivable that, in acidic solution, the Fe–porphyrin complex could decrease the overvoltage considerably. Ammonia is not a common electroreduction product although reduction of nitrite in 8 M acid, at −0.22 V, gives NH_3 with a current efficiency of ~20%.[48]

The electrocatalyzed reduction of NO to NH_3, N_2H_4, and NH_2OH in the presence of various iron complexes at pH 6 has been reported.[4b] At a potential of −1.0 V in solutions containing no catalyst, NH_3 was formed from NO with a current efficiency of ~9%, as was NH_2OH in agreement with our results for the reduction of nitrite at −0.9 V and pH 4.5. Addition of various iron complex catalysts suppresses the formation of NH_2OH and enhances the yield of ammonia which reaches a maximum con-

(44) Reference 17; p D128.

(45) Gadde, R. R.; Bruckenstein, J. *J. Electroanal. Chem. Interfacial Electrochem.* **1974**, *50*, 163.
(46) Ehman, D. L.; Sawyer, D. T. *J. Electroanal. Chem. Interfacial Electrochem.* **1968**, *16*, 541.
(47) Reference 26, p 422.
(48) Schmid, G.; Lobeck, A. *A. Elektochem.* **1969**, *73*, 189.

Table IV. Comparisons among Fe, Ru, and Os Nitrosyl Complexes

complex	$E_{1/2}(1)$, V[a]	$E_{1/2}(2)$, V[b]	pH[c]
$[Fe^{II}(NO^+)TPPS]^{3-}$	+0.35	-0.63[d]	>7
$[Ru^{II}(NO^+)(tpy)(bpy)]^{3+}$ [e]	+0.23	-0.36[f]	2.3[e]
$[Os^{II}(NO^+)(tpy)(bpy)]^{3+}$ [e]	-0.20	-0.51[f]	8.6[e]

[a] Potential for the first reduction at the nitrosyl ligand, $M-NO^+ + e^- \rightarrow M-MO^{\cdot}$. [b] Potential for the second nitrosyl-based reduction, $M-NO^{\cdot} + e^- \rightarrow M-NO^-$. [c] pH at which the nitro, $[M^{II}(NO_2)(tpy)(bpy)]^+$, and nitrosyl, $[M^{II}(NO^+)(tpy)(bpy)]^{3+}$, forms of the complex are present at equilibrium. For the Fe porphyrin the equilibrium is with free NO_2^- in solution, see text. [d] pH >2.6. [e] From ref 32. [f] Potentials are cited for pH ranges in which the wave is pH-independent.

version efficiency of about 31% with $Fe^{II}(phen)_3^{2+}$ (phen is 1,10-phenanthroline) as the catalyst.[4b] The current efficiencies quoted in this work are limited by competitive production of H_2 at the platinum electrodes used in the electrolyses.

The enzyme nitrite reductase reduces nitrite to NH_3 by a mechanism that at present is unknown. On the basis of the structural similarity between the iron isobacteriochlorin active site of the enzyme and our water-soluble iron porphyrin, it seems reasonable to suggest that the detailed redox events at the active site may be similar in detail to the events suggested in Scheme I. However, the demands on the biological system are far more complex, especially with regard to electron transfer into the heme site. Given the evidence presented here for sequential electron transfer, it is probable that the iron sulfur cluster that is associated with the iron isobacteriochlorin active site has an important role to play in providing reducing electron equivalents on demand. Related iron sulfur clusters are known to act as electron-transfer carriers in a number of biological redox systems.

Comparison of Properties Among the Fe, Ru, and Os Systems. The potentials for the first and second reductions at the nitrosyl ligand in the three complexes $[Fe^{II}(NO^+)TPPS]^{3-}$, $[Ru^{II}(NO^+)(tpy)(bpy)]^{3+}$, and $[Os^{II}(NO^+)(tpy)(bpy)]^{3+}$ and the ease with which they form nitrosyl from coordinated nitrite are compared in Table IV. Unfortunately, since we were unable to observe a complex with NO_2^- bound to the Fe(II) porphyrin, it is not possible to compare directly the acid-base equilibria that lead to nitrosyl formation. However, it is notable that $[Fe^{II}(NO^{\cdot})(TPPS)]^{4-}$ persists in solution to nearly pH 7.

Considering the dissimilar coordination environments, the similarities are remarkable. It is notable that even in the relatively electron-rich porphyrin environment, the iron porphyrin nitrosyl is the strongest of the three as an oxidant and is thermodynamically the most easily reduced at the nitrosyl ligand. This is in marked contrast to the M(III)/(II) aqua couples. The Fe(III)/(II) aqua couple at $E^{\circ\prime} = -0.23$ V is a considerable weaker oxidant than either the Ru or Os cases, for $[M(H_2O)(tpy)(bpy)]^{3+/2+}$ $E^{\circ\prime} = +0.81$ V (M = Ru) and $E^{\circ\prime} = +0.37$ V (M = Os) (25 °C) at pH 0.

The relatively high oxidizing strength for $[Fe^{II}(NO^+)(TPPS)]^{3-}$ suggests that there is considerable NO^+ character in the bound nitrosyl group and that, as compared to the Ru and Os complexes, there is considerably less $d\pi \rightarrow p\pi^*(NO)$ back-bonding.

Acknowledgments are made to the National Institutes of Health for support of this research under Grant 5-RO1-GM32296-03.

Registry No. 1, 73848-42-7; **2**, 53194-20-0; **3**, 64365-01-1; **4**, 103384-29-8; **5**, 103384-30-1; **7**, 103384-31-2; $[Fe^{II}(H_2O)_2TPPS]^{4-}$, 103384-32-3; $[Fe^{III}(H_2O)(TPPS^{\cdot+})]^{2-}$, 103384-33-4; $[Fe^{I}(TPPS)]^{5-}$, 103384-34-5; NO_2^-, 14797-65-0; NH_3, 7664-41-7; NH_2OH, 7803-49-8; N_2O, 10024-97-2; N_2, 7727-37-9; HONO, 7782-77-6.

Carbon–Carbon Bond Formation in the Reaction of Aliphatic Radicals with Alkylcobaloximes

Ron C. McHatton, James H. Espenson,* and Andreja Bakac*

Contribution from the Ames Laboratory and Department of Chemistry, Iowa State University, Ames, Iowa 50011. *Received November 25, 1985*

Abstract: Benzyl, methyl, ethyl, and isopropylaquocobaloximes, $R'Co(dmgH)_2OH_2$, react with aliphatic free radicals, R$^{\cdot}$, forming RR′ and $Co^{II}(dmgH)_2OH_2$. This reaction is quite general for aliphatic radicals, except for R = benzyl. Rate constants with R = $C(CH_3)_2OH$ and $^{\cdot}CH(CH_3)OC_2H_5$ exhibit little sensitivity toward the steric bulk of substituents on the α-carbon atom of the organocobaloxime. This discounts homolytic displacement by attack at the organic group. It is proposed that the radical addition takes place at the nitrogen end of the N=C bond of the macrocycle cis to the Co-C bond, followed by the reductive elimination of RR′.

Although homolytic displacement reactions are observed for boron, tin, and lead, authenticated examples for saturated sp^3 hybridized carbon are still quite rare.[1] Organocobaloximes[2] are good candidates to employ in a search for these rarely encountered reactions, because the leaving group is the stable cobalt(II) cobaloxime. Some examples of homolytic substitution at the saturated α-carbon atom of organometallic complexes are (i) the reaction of Cr(II) with organocobaloximes,[3a,b] eq 1, organocobalamins,[3c] and organochromium ions[4] and (ii) the alkyl transfer reactions of bis(cyclohexanedionedioximato)(pyridine)cobalt(II), $Co(chgH)_2py$, with organocobaloximes,[5] eq 2.

$$Cr^{2+}(aq) + RCo(dmgH)_2OH_2 \rightarrow (H_2O)_5CrR^{2+} + Co(dmgH)_2OH_2 \quad (1)$$

$$RCo(dmgH)_2py + Co(chgH)_2py \rightleftarrows RCo(chgH)_2py + Co(dmgH)_2py \quad (2)$$

Catalytic reactions of selected organocobaloximes with tetrahalomethanes,[6] alkylsulfonyl chlorides,[6] and arenesulfonyl chlo-

(1) Johnson, M. D. *Acc. Chem. Res.* **1983**, *16*, 343 and references therein.
(2) Cobaloxime = $Co(dmgH)_2$, where $dmgH^-$ = monanion of dimethylglyoxime (2,3-butanedionedioxime).
(3) (a) Espenson, J. H.; Shveima, J. S. *J. Am. Chem. Soc.* **1973**, *95*, 4468. (b) Bakac, A.; Espenson, J. H. *Ibid.* **1984**, *106*, 5197. (c) Espenson, J. H.; Sellers, T. D., Jr. *J. Am. Chem. Soc.* **1974**, *96*, 94.
(4) (a) Espenson, J. H.; Leslie, J. P., II. *J. Am. Chem. Soc.* **1974**, *96*, 1954. (b) Paris, M.; Ashbrook, A. W. *Can. J. Chem.* **1979**, *57*, 1233.
(5) Chrzastowski, J. Z.; Cooksey, C. J.; Johnson, M. D.; Lockman, B. R.; Steggles, P. N. *J. Am. Chem. Soc.* **1975**, *97*, 932.

0002-7863/86/1508-5885$01.50/0